

OPTICAL PROPERTIES OF ARRAYS OF GE/SI QUANTUM DOTS IN ELECTRIC FIELDS

A.V. DVURECHENSKII AND A.I. YAKIMOV
*Institute of Semiconductor Physics, SB RAS
prospekt Lavrent'eva 13, 630090 Novosibirsk, Russia*

Abstract. A photocurrent spectroscopic study of interband optical transitions in arrays of Ge/Si self-assembled quantum dots is reported. Under an applied electric field, we observe splitting of the exciton ground state, which implies that the dots possess two permanent dipole moments of opposite sign. We argue that two possible orientations of the electron-hole dipole in each Ge dot is the result of the spatial separation of electrons which can be excited in Si as well as on top and below the Ge nanocluster. The separations of electron and hole and of two electrons are determined from the observed Stark shifts. An external quantum efficiency of 1% at a telecommunication wavelength $1.3 \mu\text{m}$ was obtained for the $p-i-n$ Ge/Si quantum-dot structures.

1. Introduction

Zero-dimensional semiconductor structures [quantum dots (QDs)] display many optical phenomena known from atomic physics. One of such nice examples is the red-shift of the optical transition induced by an electric field [so called, the quantum-confined Stark effect (QCSE)]. Recent theoretical [1, 2, 3, 4] and experimental studies [5, 6, 7], reported for type-I InAs/GaAs and InGaAs/GaAs QDs, wherein the narrow-gap dot material presents a potential well for both electron and hole, demonstrated that the Stark shift can provide a very useful information on the polarity of intra- and interdot electron-hole alignment and the vertical separation.

The change of the potential energy of a dipole with a moment \mathbf{p} in an electric field \mathbf{F} is given by $U = -\mathbf{p}\mathbf{F}$ (Ref. [8]). For the electron-hole system, $\mathbf{p} = e(\langle\mathbf{r}_h\rangle - \langle\mathbf{r}_e\rangle)$, where $\langle\mathbf{r}_{e,h}\rangle$ is the mean electron (hole) position. In type-II QDs, only one of the charge carriers is confined inside the dot

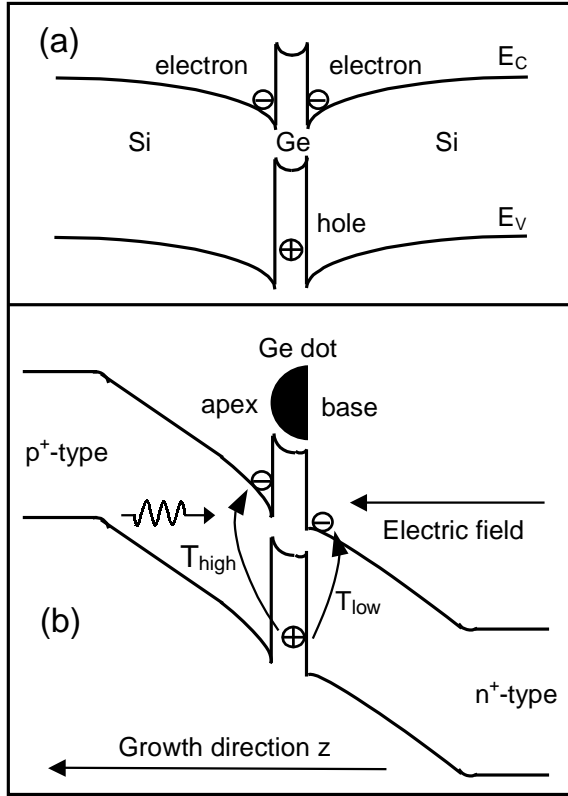


Figure 1. (a) Band structure of the type-II Si/Ge/Si heterostructure along the growth direction through the center of the Ge dot. (b) Schematic band diagram of the $p-i-n$ diode under reverse bias.

whereas another carrier resides outside the dot. In contradistinction with the case of type-I QDs, one can expect that in such a system the Stark effect should be an extremely large because of the permanent spatial separation of electron and hole and the presence of the built-in electron-hole dipole [4]. To date, most work in the field of QCSE has concentrated on InAs/GaAs QDs, and very little is known about the influence of electric field on the excitonic properties of type-II QDs. It is generally accepted that Ge/Si(004) quantum dots exhibit a type-II band lineup [9, 10, 11]. When an electron-hole pair is photoexcited, the hole is captured into the quantum well of the Ge dot and creates an attractive Coulomb potential resulting in a binding of an electron in Si [Fig. 1(a)] at the Si/Ge interfaces and forming the spatially indirect excitons. In present work we use photocurrent (PC) spectroscopy to study the effect of an electric field on the interband transitions in Ge/Si(001) quantum dots.

2. Experimental

For controlled tuning of the electric field, the Ge QDs are embedded in the intrinsic region of an Si $p-i-n$ diode (p^+ region uppermost), allowing fields up to 90 kV/cm to be applied parallel to the growth direction z (applying a reverse bias to a $p-i-n$ structure results in an electric field pointing from n^+ substrate to p^+ surface). The band profile under reverse bias condition is shown schematically in Fig. 1(b).

To observe experimentally the QCSE by PC spectroscopy, it is necessary the two conditions to be fulfilled. First, the size of the dots in all three dimensions should be small enough to provide actual zero-dimensional density of states. Second, the electron and hole must be well separated to ensure the large dipole moment, so the dots should be rather tall. However, conventional Ge/Si(001) self-assembled QDs, grown by Stranskii-Krastanov growth techniques, are always flat and have an aspect ratio much less than unity [12]. To fabricate tall Ge islands with small lateral size, we grow the Ge dots on a Si(001) substrate covered with ultrathin SiO_x film. Recently similar approach has been successfully applied to form high-density ultra-small Ge islands on Si(111) [13] and Si(001) [14] surfaces. The mechanism of Ge nanocluster formation on the ultrathin SiO_x films was essentially different from that on clean Si surfaces and is beyond the scope of this paper. A possible hypothesis has been put forward by Shklyaev and co-workers [13] and takes into account a reaction between individual Ge adatoms and SiO_x followed by a local silicon oxide desorption. The reflection-high-energy-electron-diffraction (RHEED) data show that three-dimensional Ge islands are appeared without the formation of a wetting layer and exhibit an epitaxial relationship with the underlying silicon substrate. The latter observation implies that, similar to the case of Stranski-Krastanov islands, Ge nanoclusters fabricated on oxidized Si surface reside on *bare* Si regions.

The sample was grown by molecular-beam epitaxy at a temperature of 500°C on an n^+ -Si(001) substrate ($7 \times 10^{17} \text{ cm}^{-3} \text{ As}$). The growth rates were 2 ML/s for Si and 0.2 ML/s for Ge. For $p-i-n$ structures 400-nm i -Si region was first grown. To oxidize the surface, the oxygen had been introduced into the chamber at a pressure of 10^{-4} Pa for 10 min. After oxygen was pumped out and the chamber pressure reached 10^{-7} Pa , nominally, 1 nm of Ge was deposited. The growth of the QDs is followed by 400 nm i -Si and 200 nm p^+ -doped Si layer ($2 \times 10^{18} \text{ cm}^{-3} \text{ B}$). The structure was finally capped with a 10 nm of p^+ -Si contact layer ($10^{19} \text{ cm}^{-3} \text{ B}$). The background boron concentration in the intentionally undoped i -Si layers was $(7 - 8) \times 10^{15} \text{ cm}^{-3}$. The QDs formation and quality of the silicon grown to embed the dots was controlled *in situ* by RHEED. It was establish that despite the presence of the silicon dioxide layer, the cap silicon is also single crystal.

Rectangular mesa diodes with areas ranging from 2.5×10^{-4} to 5×10^{-4} cm² were fabricated by standard lithography and wet chemical etching. A 100 nm SiO₂ passivation layer was deposited by chemical vapor deposition. The ohmic contacts with the p^+ and the n^+ layers were obtained by depositing 80×80 μm² Al contacts.

The layer of QDs capped with a 10-nm-thick Si layer was examined with plan-view and cross-sectional electron microscopy (Fig. 2) [15, 16]. The Ge islands have a hemispherical shape with a base diameter of 5.8 ± 0.5 nm and a height of about 3–4 nm. The apex of the dots is oriented along the growth direction. The areal density of the islands was approximately 1.8×10^{12} cm⁻². To separate photoresponse from the dots, the reference sample was grown under conditions similar to the dot sample, except that no Ge was deposited.

It is necessary to note that when the nominal thickness of Ge layer reaches 1 nm, distribution of Ge dot sizes becomes bimodal. Along with the ultrasmall high-density islands, very large low-density ($\sim 10^8$ cm⁻²) lens-shaped Ge nanocrystals (≈ 200 nm in diameter and ≈ 40 nm in height) appear. However, as we will argue at the end of the paper, these islands cannot be responsible for the measured PC spectra.

PC measurements were performed in normal-incidence geometry (incident light polarized in the plane of the samples) at room temperature. Short circuit (no bias) photocurrent was directly measured with a Keithley electrometer. For biased measurements, a lock-in amplifier was used. In the latter case, the light from global source was mechanically chopped at the frequency of about 550 Hz. Low illumination power density of ~ 0.1 mW cm⁻² was employed to provide an extremely low dot carrier occupancy and to avoid many-particle effects. In order to obtain the responsivity of the $p-i-n$ diode, the spectral photon flux from the light source was measured by using a calibrated pyroelectric detector.

3. Results and Discussion

Figure 3 shows photocurrent spectra as a function of reverse bias. There is apparent PC peak below the silicon interband absorption edge (1126 eV) which is not seen in the reference sample (crosses in Fig. 3). At low bias, peak at ≈ 1040 meV has a symmetric line shape and is believed to come from the indirect excitonic transition between the hole ground state in the Ge dots and the electron ground state confined in Si near the heterojunction. The electron-hole pairs created by interband absorption thermally escape from the dots and give rise to the measured photocurrent. As the reverse bias increases, the current maximum becomes wider and splits into two peaks which are changed with the applied voltage in a different way.

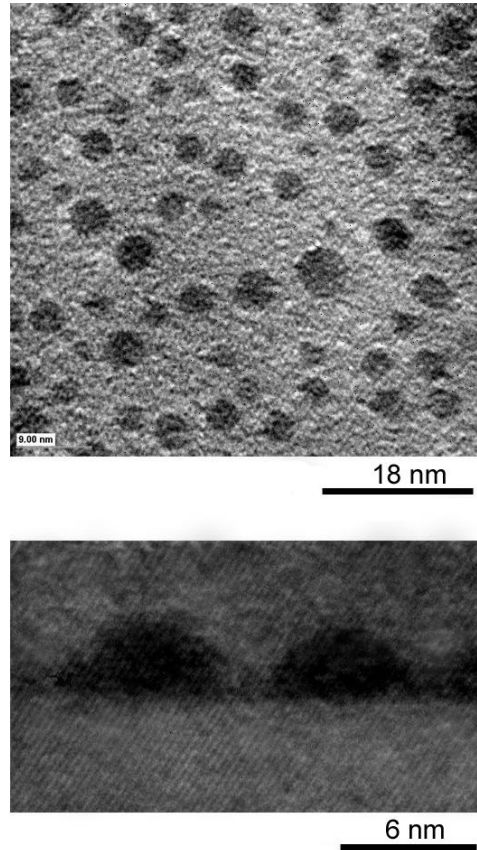


Figure 2. Plan-view (top) and cross-section (bottom) transmission electron microscopy images of a 1-nm Ge dot sample. The Ge islands appear in dark contrast.

Position of the low-energy peak T_{low} is practically unchanged with the bias while the high-energy component T_{high} apparently shifts to *higher* energies.

To explain splitting and the blueshift of the high-energy transition, one needs to consider the electronic structure of excitons in type-II Ge/Si QDs. The modeling of the confined electron and hole states [9, 10] predicts that holes are concentrated at the bottom of the dot, and the electrons are localized in Si both on top and below the Ge island. This is the result of strain distribution and Coulomb forces around the dot. Recently the confirmation of the spatial separation of electrons in the silicon matrix surrounding the Ge islands was provided by observation of a negative interband photoconductivity in *n*-type Ge/Si(001) QDs [17].

It follows from the second-order perturbation theory that the field de-

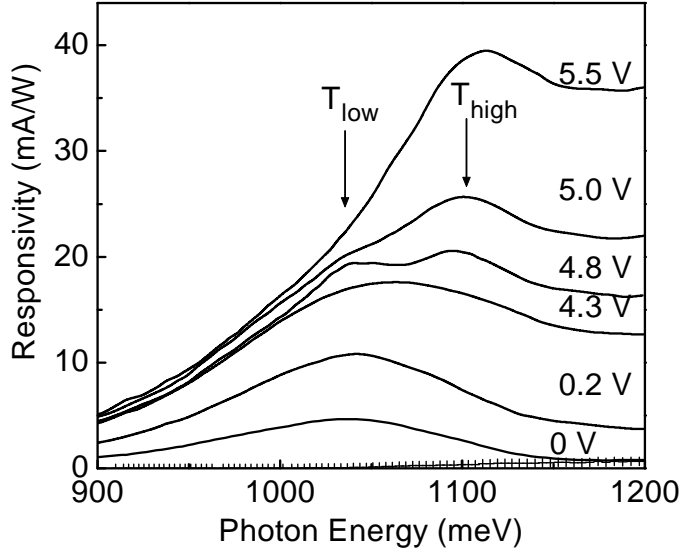


Figure 3. Photocurrent spectra as a function of applied reverse bias (lines). The nominal Ge coverage is 1 nm. The short circuit photoresponse from a reference Si photodiode is shown by crosses.

pendence of the transition energy can be described by

$$E(F) = E(0) - eF(\langle z_h \rangle - \langle z_e \rangle) - \beta F^2, \quad (1)$$

where $e = -|e|$ is the electron charge, $E(0)$ is the transition energy at zero field, $\langle z_{e,h} \rangle$ is the mean electron (hole) position along the growth direction (along the nanocrystal axis), β is the polarizability of the electron-hole system [2]. In a system possessing a nonzero dipole moment, the second order term in Eq. (1), quadratic in the applied field, must be less important than a linear one and the transition energy must vary linearly with the field.

In framework of this conception, we interpret the high-energy maximum T_{high} as a transition between the hole ground state in the Ge dot and the electron state confined in Si near the dot apex [16]. The low-energy peak T_{low} is assigned to the transition between the same hole state and the electron state localized in Si near the dot base [see Fig. 1(b)]. Obviously, the term $eF(\langle z_h \rangle - \langle z_e \rangle)$ is negative for the first case and positive for the second one since the electron-hole dipoles formed as a result of the T_{high} and T_{low} transitions have the opposite directions.

We can check our explanation by extracting the values of electron-hole and electron-electron separation from the observed Stark shift. First, keeping in mind that the observed PC maximum is a superposition of the two peaks, we decompose the maximum into two Gaussians. This allowed us

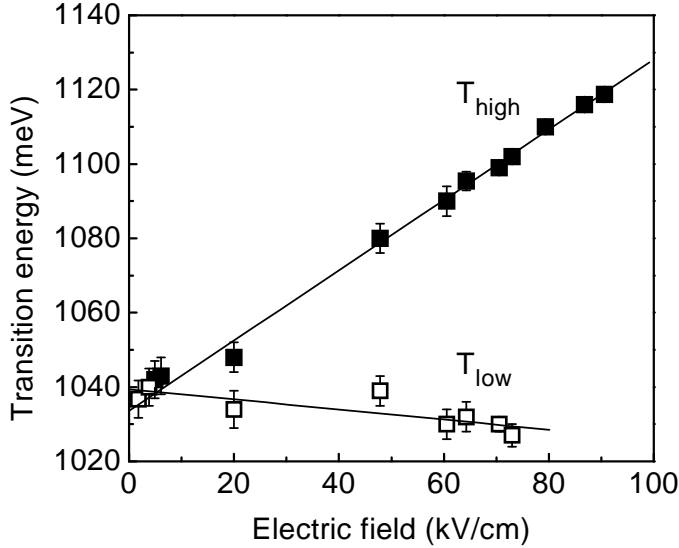


Figure 4. Transition energies as a function of electric field for 1-nm-Ge sample. The solid lines are theoretical fits to the experimental data.

to determine the transition energies. Then we made a self-consistent one-dimensional simulation of our $p-i-n$ device to calculate the electric field near the apex and the base of the dots.

The field dependence of the transition energies are plotted in Fig. 4. As expected for a system with built-in dipole moments, the Stark shift for both transitions appears to be linear. Moreover, due to the linear behavior, the type-II Ge/Si QDs exhibit a QCSE of approximately one order-of-magnitude stronger than type-I InGaAs/GaAs QDs of similar height[7]. From a fit to the data using the Eq. (1), we find the electron-hole distance (5.1 ± 0.2) nm for the electron near the dot apex (top electron) and $-(0.8 \pm 0.3)$ nm for the electron near the dot base (bottom electron). It is worth to note that separation of these two electrons (≈ 6 nm) is somewhat larger than the mean dot height (≈ 4 nm), which is quite reasonable for QDs with a staggered band line-up providing clear support for the our explanation. Moreover, the small separation of the bottom electron and the hole agrees with the fact that hole is localized towards the base of the dots.

To obtain further evidence to support the QD related origin of the PC maxima, we have fabricated another test sample grown under conditions similar to the previous dot sample, except that 2 nm Ge was deposited. This produced smaller Ge dots (about 4 nm in diameter and 2 nm in height) with somewhat larger areal density ($2 \times 10^{12} \text{ cm}^{-2}$). Due to stronger hole confinement in small dots, the excitonic transition is shifted to higher

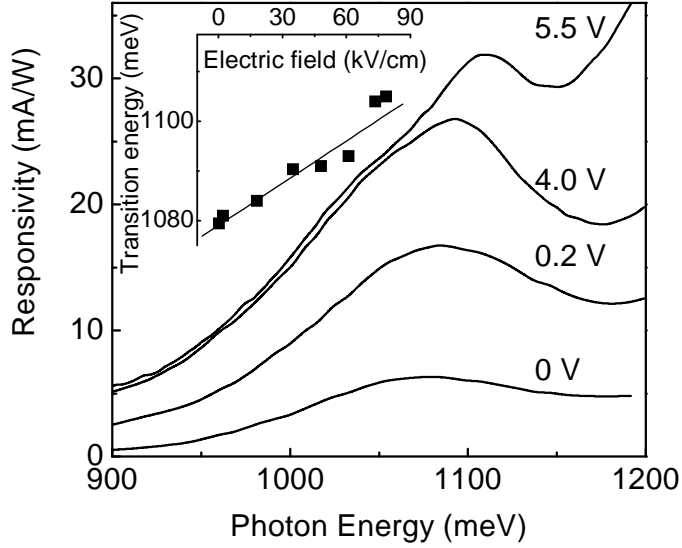


Figure 5. Photocurrent spectra as a function of applied reverse bias for a sample with a nominal Ge coverage of 2 nm. The inset shows the high-energy transition energy as a function of electric field.

energies as compared with the 1-nm Ge structure (Fig. 5). Also, since the dots are thinner, the Stark effect is rather small. From the dependence of the transition energy on the electric field (inset of Fig. 5), we deduce the top electron-hole separation of 2.5 ± 0.8 nm, again in agreement with the dot height.

We now focus attention on the variation of the PC intensity with electric field. The amplitude of the low-energy signal increases with increasing F at low fields and saturates at bias $V \geq 5$ V. The intensity of the high-energy maximum continues to increase even at highest F . The increasing value of both PC peaks at low F can be related to an increasing rate of carrier escape with F . By applying a reverse bias, the electric field push the top electron towards the hole in the dot and pull the bottom electron out from the hole. As a consequence, the electron-hole overlap and the corresponding absorption strength are increased for the T_{high} transition and reduced for the T_{low} transition. At highest F , no bound state can further exist for the bottom electron and the T_{low} transition transforms into a PC tail on the low-energy side of the T_{high} absorption.

Next let us discuss the possible role of huge Ge islands which present in the structures. We claim that these islands are of no importance for observed PC spectra, adducing the following arguments. First, the maximum external quantum efficiency η of the investigated photodiodes deduced from the responsivity is about 1% at a telecommunication wavelength $1.3 \mu\text{m}$ (at

953 meV). Similar value of η (2.3%) was achieved in Ge/Si quantum-dot waveguide photodetector, which contains five layers of Ge islands with a density of $3 \times 10^9 \text{ cm}^{-2}$ in each layer and was designed to have a *strong optical confinement* [18]. Obviously, one layer of Ge islands having a very low density ($2 \times 10^8 \text{ cm}^{-2}$ for large islands in 1-nm Ge sample and $5 \times 10^8 \text{ cm}^{-2}$ for 2-nm Ge sample) cannot ensure a measurable PC, especially at normal incidence. This is possible only for an extremely high-density QD structure. Second, 100-nm-sized Ge/Si self-assembled islands usually exhibit an exciton related photoluminescence peak around $\sim 800 \text{ meV}$ (see Ref. [19] and references therein). To provide the excitonic transition at larger energies (1040–1100 meV), the ultrasmall Ge QDs with enhanced size quantization of the hole energy spectrum are required.

4. Summary and Conclusions

In summary, the photocurrent spectroscopy of type-II Ge/Si(001) quantum dots, as a function of applied electric field, has demonstrated that the QDs possess two built-in electric dipoles of opposite orientations. We argue that this is a consequence of the spatial separation of the electrons around the dots. From the observed Stark shift, both separation of the electrons and hole at the dots and the distance between the electrons were determined. We found that, due to the linear behavior, the type-II Ge/Si QDs exhibit a QCSE of approximately one order-of-magnitude stronger than type-I InGaAs/GaAs QDs. An external quantum efficiency of about 1% at $1.3 \mu\text{m}$ of wavelength was obtained at room temperature. This result indicates that the Ge/Si QDs are potentially applicable for Si-based $1.3\text{--}1.5 \mu\text{m}$ optical fiber communication.

Acknowledgments. The authors are much obliged to A. Milekhin and S. Schulze for TEM measurements, A. O. Govorov for helpful discussion, A. V. Nenashev for self-consistent calculations, N. P. Stepina for assistance in sample preparation, and I. B. Chistoknin for technical assistance. This work was supported by the RFBR, the Education Ministry program (grant E00-3.4-154) and INTAS-2001-0615.

References

1. Li, S.-S. and Xia, J.-B. (2000) Quantum-confined Stark effects of InAs/GaAs self-assembled quantum dot, *J. Appl. Phys.* **88**, pp. 7171–7174.
2. Barker, J.A. and O'Reilly, E.P. (2000) Theoretical analysis of electron-hole alignment in InAs-GaAs quantum dots, *Phys. Rev. B* **61**, pp. 13840–13851.
3. Sheng, W. and Leburton, J.-P. (2002) Anomalous quantum-confined Stark effects in stacked InAs/GaAs self-assembled quantum dots, *Phys. Rev. Lett.* **88**, art. no. 1674401.
4. Janssens, K.L., Partoens, B., and Peeters, F.M. (2002) Stark shift in single and vertically cccoupled type-I and type-II quantum dots, *Phys. Rev. B* **65**, art. no.

- 233301.
5. Fry, P.W., Itskevich, I.E., Mowbray, D.J., Skolnick, M.S., Finley, J.J., Barker, J.A., O'Reilly, E.P., Wilson, L.R., Larkin, I.A., Maksum, P.A., Hopkinson, M, Al-Khafaji, M., David, J.P.R., Cullis, A.G., Hill, G., and Clark, J.C. (2000) Inverted electron-hole alignment in InAs-GaAs self-assembled quantum dots, *Phys. Rev. Lett.* **84**, pp. 733–736.
 6. Patanè, A., Levin, A., Polimeni, A., Schindler, F., Main, P.C., Eaves, L., and Henini, M. (2000) Piezoelectric effects in $\text{In}_{0.5}\text{Ga}_{0.5}\text{As}$ self-assembled quantum dots grown on (311)*B* GaAs substrates, *Appl. Phys. Lett.* **77**, pp. 2979–2981.
 7. Findeis, F., Baier, M., Beham, E., Zrenner, A., and Abstreiter, G. (2001) Photocurrent and photoluminescence of a single self-assembled quantum dot in electric fields, *Appl. Phys. Lett.* **78**, pp. 2958–2960.
 8. Sacra, A., Norris, D.J., Murray, C.B, and Bawendi, M.J. (1995) Stark spectroscopy of CdSe nanocrystallites: The significance of transition linewidth, *J. Chem. Phys.* **103**, pp. 5236–5245.
 9. Yakimov, A.I., Stepina, N.P., Dvurechenskii, A.V., Nikiforov, A.I., Nenashev, A.V. (2000) Excitons in charged Ge/Si type-II quantum dots, *Semicond. Sci. Technol.* **15**, pp. 1125–1130; Interband absorption in charged Ge/Si type-II quantum dots, *Phys. Rev. B* **63**, art. no. 045312.
 10. Schmidt, O.G., Eberl, K., and Rau, Y. (2000) Strain and band-edge alignment in single and multiple layers of self assembled Ge/Si and GeSi/Si islands, *Phys. Rev. B* **62**, pp. 16715–16720.
 11. Cusack, M.A., Briddon, P.R., North, S.M., Kitchin, M.R., and Jaros, M. (2001) Si/Ge self-assembled quantum dots for infrared applications, *Semicond. Sci. Technol.* **16**, pp. L81–L84.
 12. Pchelyakov, O.P., Bolhovityanov, Yu.B., Dvurechenskii, A.V., Nikiforov, A.I., Yakimov, A.I., and Voigtländer, B. (2000) Molecular beam epitaxy of silicon-germanium nanostructures, *Thin Solid Films* **362**, pp. 75–84.
 13. Shklyae, A.A., Shibata, M., and Ichikawa, M. (2000) High-density ultrasmall epitaxial Ge islands on Si(111) surfaces with a SiO_2 coverage, *Phys. Rev. B* **62**, pp. 1540–1543.
 14. Barski, A., Derivaz, M., Rouvière, J.L., and Buttard, D. (2000) Epitaxial growth of germanium dots on Si(001) surface covered by a very thin silicon oxide layer, *Appl. Phys. Lett.* **77**, pp. 3541–3543.
 15. Milekhin, A.G., Nikiforov, A.I., Pchelyakov, O.P., Galzerani, J.C., Schulze, S., and Zahn, D.R.T. (2002) Resonant Raman scattering of relaxed Ge quantum dots, in *Proceedings of the 26th International Conference on the Physics of Semiconductors*. Edinburgh, Scotland.
 16. Yakimov, A.I., Dvurechenskii, A.V., Nikiforov, A.I., Ul'yanov, V.V., Milekhin, A.G., Schulze, S., and Zahn, D.R.T. (to be published).
 17. Yakimov, A.I., Dvurechenskii, A.V., and Nikiforov, A.I. (2001) Spatial separation of electrons in Ge/Si(001) heterostructures with quantum dots, *JETP Lett.* **73**, pp. 529–531.
 18. El kurdi, M., Boucaud P., Sauvage, S., Fishman, G., Kermarrec, O., Campidelli, Y., Bensahel, D., Saint-Girons, G., Sagnes, I., and Patriarche, G. (2002) Silicon-insulator waveguide photodetector with Ge/Si self-assembled islands, *J. Appl. Phys.* **92**, pp. 1858–1861.
 19. Pchelyakov, O.P., Bolkhovityanov, Yu. B, Dvurechenski, A.V., Sokolov, L.V., Nikiforov, A.I., Yakimov, A.I., and Voigtlander, B. (2000) Silicon-Germanium Nanostructures with Quantum Dots: Formation Mechanisms and Electrical Properties, *Semiconductors* **34**, pp. 1229–1247.